

Nonequilibrium phenomena in nonlinear lattices: from slow relaxation to anomalous transport

Stefano Iubini, Stefano Lepri, Roberto Livi, Antonio Politi, and Paolo Politi

Abstract This Chapter contains an overview of the effects of nonlinear interactions in selected problems of non-equilibrium statistical mechanics. Most of the emphasis is put on open setups, where energy is exchanged with the environment. With reference to a few models of classical coupled anharmonic oscillators, we review anomalous but general properties such as extremely slow relaxation processes, or non-Fourier heat transport.

Stefano Iubini
Dipartimento di Fisica e Astronomia, Università di Padova, via F. Marzolo 8 I-35131, Padova, Italy e-mail: stefano.iubini@unipd.it

Stefano Lepri
Consiglio Nazionale delle Ricerche, Istituto dei Sistemi Complessi, via Madonna del Piano 10, I-50019 Sesto Fiorentino, Italy e-mail: stefano.lepri@isc.cnr.it
Istituto Nazionale di Fisica Nucleare, Sezione di Firenze, via G. Sansone 1 I-50019, Sesto Fiorentino, Italy

Roberto Livi
Dipartimento di Fisica e Astronomia, Università di Firenze, via G. Sansone 1 I-50019, Sesto Fiorentino, Italy e-mail: roberto.livi@unifi.it
Istituto Nazionale di Fisica Nucleare, Sezione di Firenze, via G. Sansone 1 I-50019, Sesto Fiorentino, Italy
Consiglio Nazionale delle Ricerche, Istituto dei Sistemi Complessi, via Madonna del Piano 10, I-50019 Sesto Fiorentino, Italy

Antonio Politi
Institute for Pure and Applied Mathematics & SUPA University of Aberdeen, Aberdeen AB24 3UE, Scotland, United Kingdom e-mail: a.politi@abdn.ac.uk

Paolo Politi
Consiglio Nazionale delle Ricerche, Istituto dei Sistemi Complessi, via Madonna del Piano 10, I-50019 Sesto Fiorentino, Italy e-mail: paolo.politi@isc.cnr.it
Istituto Nazionale di Fisica Nucleare, Sezione di Firenze, via G. Sansone 1 I-50019, Sesto Fiorentino, Italy

1 Introduction

The title of this Chapter contains two negations, *nonequilibrium* and *nonlinearity*, which signal a double source of difficulties. First, at variance with equilibrium statistical mechanics, there is no general approach to describe the evolution of a generic system far from equilibrium. Second, nonlinear forces notoriously have to be handled with care.

From the fundamental point of view, nonlinear interactions are essential for the theoretical foundations of irreversible processes: a derivation of phenomenological relations (like for instance Fourier's law) from microscopic dynamics is indeed one of the challenges of mathematical physics. On the other hand, understanding the role of nonlinearity, low-dimensionality, long-range interactions, disorder etc. may help developing innovative ideas for nanoscale thermal management with possible future applications like controlling the heat fluxes in small devices built on molecular junctions, carbon nanotubes, polymers and nano-structured materials [1].

This Chapter aims at illustrating the combined effect of nonlinear interactions on relaxation and transport: since this is an exceedingly vast topic, we focus mainly on selected specific issues. In particular, we wish to review through some examples (mostly relying on numerical simulations) of how relaxation and transport are affected by nonlinear interactions in systems of classical nonlinear oscillators. This class of model represents a large variety of different physical problems like atomic vibrations in crystals and molecules or field modes in optics or acoustics.

The Chapter is organized as follows. For concreteness, we discuss mostly one-dimensional arrays of classical oscillators, that are reviewed in Section 2. For later purposes, their equilibrium thermodynamics is recalled in Section 3. Section 4 deals with the typical times-scales of relaxation to a steady state in the presence of a dissipation applied to the boundaries and discuss how nonlinear localization can significantly affect the process. This is the most detailed section, since the topic is still open and we have preferred to add some recent details for the sake of clarity. In Section 5 we address the issue of nonequilibrium steady states for chains in contact with different thermal reservoirs. We recall there how nonlinear interactions affect fluctuations of conserved quantities and conspire to yield energy superdiffusion. Finally, in Section 6 we outline possible future developments.

2 Classical coupled nonlinear oscillators: basic models

A vast number of micro- and mesoscopic models have been introduced and studied to understand nonequilibrium dynamics. Many of them involve some form of stochasticity [2]. Here we concentrate on open Hamiltonian models described by unidimensional arrays of N classical nonlinear oscillators. Two

families of models are reviewed: (i) separable systems characterized by kinetic and potential energy; (ii) non-separable ones such as the the Discrete Nonlinear Schrödinger (DNLS) equation.

The first class is generally characterized by the Hamiltonian

$$H = \sum_{n=1}^N \left[\frac{p_n^2}{2m} + U(q_n) + V(q_{n+1} - q_n) \right] , \quad (1)$$

where q_n and p_n denote position and momentum of the point-like particles; m is their mass while the potential $V(x)$ accounts for the nearest-neighbour interactions between consecutive particles, and, finally, the on-site potential $U(q_n)$ accounts for the possible interaction with an external environment (e.g., a substrate).

The corresponding evolution equations are

$$m\ddot{q}_n = -U'(q_n) - F(r_n) + F(r_{n-1}) \quad , \quad n = 1, \dots, N, \quad (2)$$

where $r_n = q_{n+1} - q_n$, $F(x) = -V'(x)$, and the prime denotes a derivative with respect to the argument. If q_n denotes a longitudinal position, then $L = \sum_{n=1}^{N-1} r_n$ represents the total length of the chain, which, in the case of fixed boundary conditions (b.c.), is a constant of motion. Conversely, if the particles are confined in a simulation “box” of length L with periodic b.c., we have $q_{n+N} = q_n + L$. Alternatively, one can adopt a lattice interpretation whereby the (discrete) position is $x_n = an$ (where a is the lattice spacing), while q_n is a transversal displacement. Thus, the chain length is obviously equal to Na .

For isolated systems, the Hamiltonian (1) is a constant of motion. If the pinning potential U is constant, the total momentum $P = \sum_{n=1}^N p_n$ is conserved, as well. Since we are interested in heat transport, one can set $P = 0$ (i.e., we assume to work in the center-of-mass reference frame) without loss of generality. As a result, the relevant state variables of microcanonical equilibrium are the specific energy (i.e., the energy per particle) $h = H/N$ and the elongation $\ell = L/N$ (i.e., the inverse of the particle density).

An important subclass is the one in which V is quadratic, which can be regarded as a discretization of the Klein-Gordon field: relevant examples are the Frenkel-Kontorova [3, 4] and “ ϕ^4 ” models [5, 6] which, in suitable units, correspond to $U(y) = 1 - \cos(y)$ and $U(y) = y^2/2 + y^4/4$, respectively. Another toy model that has been studied in some detail is the ding-a-ling system [7], where U is quadratic and the nearest-neighbor interactions are replaced by elastic collisions.

2.1 The Fermi-Pasta-Ulam-Tsingou chain

In this context, the most paradigmatic example is the Fermi–Pasta–Ulam–Tsingou (FPUT) model, with $U(q_n) = 0$ and

$$V(r_n) = \frac{k_2}{2} (r_n - a)^2 + \frac{k_3}{3} (r_n - a)^3 + \frac{k_4}{4} (r_n - a)^4 \quad , \quad (3)$$

introduced in a widely acknowledged seminal work [8] in nonlinear dynamics. It is well known that the initial goal of the study was to demonstrate that a generic nonlinear interaction should eventually drive an isolated mechanical system with many degrees of freedom, towards an equilibrium state characterised by energy equipartition among normal modes. Actually, in the following decades the related problem of steady state transport was also considered [9, 10, 11].

Following the notation of the original work [8], the coupling terms k_3 and k_4 are denoted by α and β , respectively; historically this model is sometimes referred to as the “FPU- $\alpha\beta$ ” model. In the absence of the cubic nonlinearity ($k_3 = 0$), the system is referred to as “FPU- β ” model. Notice that upon introducing the displacement $u_n = q_n - na$ from the equilibrium position, r_n can be rewritten as $u_{n+1} - u_n + a$, so that the lattice spacing a disappears from the equations.

2.2 The Discrete nonlinear Schrödinger equation

The Discrete Nonlinear Schrödinger (DNLS) equation has been widely investigated in various domains of physics as a prototype model for the propagation of nonlinear excitations [12, 13, 14]. Originally, it was proposed to describe electronic transport in biomolecules [15] and later for nonlinear wave propagation in photonic or phononic crystals [16, 17] as well as in ultra-cold atom gases in optical lattices [18].

The system (in its dimensionless form) is described by the Hamiltonian

$$H = \sum_{n=1}^N (|z_n|^4 + z_n^* z_{n+1} + z_n z_{n+1}^*) \quad (4)$$

where the complex variables z_n and $-iz_n^*$ ($n = 1, \dots, N$) are canonical variables. The Hamilton equations $\dot{z}_n = -\partial H / \partial (iz_n^*)$ are written as

$$i\dot{z}_n = -2|z_n|^2 z_n - z_{n-1} - z_{n+1} \quad . \quad (5)$$

Sometimes it is convenient to decompose z_n into real and imaginary components: $z_n = (p_n + iq_n)/\sqrt{2}$; this way q_n and p_n are standard conjugate

canonical variables. Besides the Hamiltonian, the system admits a second constant of motion, namely the total norm $A = \sum_{n=1}^N |z_n|^2$ which, depending on the physical context, can be interpreted as the gas particle number, optical power, etc. At variance with its continuum counterpart, the DNLS is non-integrable: it typically displays a chaotic dynamics.

A peculiarity of this model is the existence of localized solutions, the so-called *discrete breathers* (DB) [14, 19], characterized by a large amplitude on a single site, $|z_n|^2 \gg s^2$, where s^2 is the amplitude of the surrounding background. In the limit of $s \ll 1$, when perturbative calculations can be carried out, the long term stability has been discussed in full detail [20]. We later on show that breather stability is an important issue also in physical setups, where the background is fully chaotic.

2.3 The coupled rotors model

Another interesting system is the coupled rotors chain described by the equations of motion

$$\dot{q}_n = p_n, \quad \dot{p}_n = \sin(q_{n+1} - q_n) - \sin(q_n - q_{n-1}). \quad (6)$$

This model is sometimes referred to as the Hamiltonian version of the XY spin chain. It is a sort of intermediate model between standard oscillator chains (notice that here the “position” q_n is an angle) and the DNLS equation, once we think of the variable z_n as composed of amplitude and phase. In fact, it can be shown that in some limit the DNLS reduces to a rotor chain [21].

3 Equilibrium

Equilibrium thermodynamics of the above models can be calculated by standard means. For the Hamiltonian (1) without pinning ($U = 0$) this can be accomplished straightforwardly by computing the partition function in the isobaric ensemble [22]. For models like Klein-Gordon and DNLS lattices, the computation requires the use of transfer integral methods [23].

The case of the DNLS is of particular interest: a thermodynamic equilibrium state is in fact specified by two intensive parameters, the mass density $a = A/N \geq 0$ and the energy density $h = H/N$ or equivalently by the conjugate variables μ (chemical potential) and β (inverse temperature). The equilibrium phase-diagram in the (a, h) plane [23] is bounded from below by the ($T = 0$) ground-state line $h = a^2 - 2a$ corresponding to a uniform state with constant amplitude and constant phase-differences $z_n = \sqrt{a}e^{i(\mu t + \pi n)}$, with $\mu = 2(a - 1)$. States below this curve are not physically accessible.

The positive-temperature region lies between the ground-state line and the infinite-temperature ($\beta = 0$) line, given by $h = 2a^2$. In this limit, the grand-canonical equilibrium distribution becomes proportional to $\exp(\beta\mu A)$, where the finite (negative) product $\beta\mu$ implies a diverging chemical potential. Equilibrium states at infinite temperature are therefore characterized by an exponential distribution of the amplitudes, $P(|z_n|^2) = a^{-1}e^{-|z_n|^2/a}$ and random phases. Finally, states above the $\beta = 0$ line belong to the so-called negative-temperature region [23, 24]. From a thermodynamic point of view, the presence of states at absolute negative temperature is a consequence of the entropy being a decreasing function of the internal energy. Very recently it has been found that this region is characterized by inequivalence of statistical ensembles [25]. While just above the $\beta = 0$ line the microcanonical partition function can be computed explicitly by large-deviation techniques, the grand-canonical partition function is undefined, due to the presence of a branch-cut singularity in the complex β -plane. Moreover, the microcanonical ensemble predicts the presence of a first-order phase transition from a thermalized phase, below the $\beta = 0$ line, to a condensed phase, above the $\beta = 0$ line. This situation represents a typical scenario of broken ergodicity in the negative-temperature phase, induced by a condensation phenomenon, due to the spontaneous formation and coalescence of DB.

Since the DNLS Hamiltonian (4) is not separable, one cannot determine temperature and chemical potential via the standard molecular-dynamics tools. It is necessary to make use of the microcanonical definition provided in [26]. The general expressions are nonlocal and rather involved; we refer to [27] for details and the related bibliography. Alternatively, one can determine the relations $a(T, \mu)$, $h(T, \mu)$ numerically, by putting the system in interaction with an external reservoir that imposes T and μ and by measuring the corresponding equilibrium densities.¹

4 Relaxation

In this section we review and discuss relaxation dynamics, namely how the equilibrium steady state is reached starting from nonequilibrium initial conditions. Generally speaking one may distinguish between two cases:

¹ The actual implementation of a reservoir for the DNLS is less straightforward than for usual oscillator models [28]. Two main strategies have been proposed: the first is a Monte-Carlo dynamics [27] whereby the reservoir performs random perturbations δz_1 of, say, the state variable z_1 that are accepted or rejected according to a grand-canonical Metropolis cost-function $\exp[-\beta(\Delta H - \mu\Delta A)]$, where ΔH and ΔA are respectively the variations of energy and mass produced by δz_1 . Between successive interactions with the environment the dynamics is Hamiltonian and can be integrated by symplectic algorithms [29]. Another approach is based on a Langevin dynamics with a dissipation designed in such a way that equilibrium corresponds to the grand-canonical measure [24].

- (i) relaxation to thermal equilibrium (energy equipartition) from a particular initial state in the *isolated* (microcanonical) setup;
- (ii) evolution towards a steady state in an *open* setup, whereby the system is allowed to exchange energy, momentum etc. with the environment, composed of one (or more) reservoirs.

A typical example of case (i) is the numerical experiment discussed in the original FPUT paper, a problem deeply related to the validity of the ergodic hypothesis. In the following, we will not dwell further on the FPUT problem: the interested reader can look at some recent literature [30, 31, 32]. Here, we focus more on boundary-induced relaxation phenomena with a particular emphasis given to the DNLS, for the existence of a negative-temperature region.

4.1 *Localization by boundary cooling*

A first numerical evidence of slow-relaxation induced by the spontaneous emergence of localized inhomogeneities has been provided by Tsironis and Aubry [33], who discussed the chain dynamics in the presence of a nonlinear pinning potential. The system, initially prepared in a thermalized state at some given temperature T , was put in contact with a cold (zero temperature) heat bath, by adding a damping term on a few boundary particles. The chain eventually converges to a quasi-stationary state, where a residual amount of energy is kept under the form of a few isolated DBs. It has been later argued that the energy relaxation obeys a stretched exponential law in time [34, 35].

The rotor model is yet another interesting example where boundary dissipation leads to a slow relaxation. In Ref. [36] it was found that for long enough times the energy decreases very slowly, according to a typical stretched-exponential law

$$E(t) = E(0) \exp(-(t/\tau)^\sigma)$$

with $\sigma < 1$ (typically $\sigma \approx 0.5$) and τ being some characteristic timescale. The occurrence of slow dynamics has been associated with a progressive destruction of localized excitations (the so-called rotobreathers) and energy release at the boundaries. At very long times a residual quasi-stationary state is again observed: a finite fraction of the initial energy is stored into a single rotobreather and remains constant over the rest of the simulation.

Recently, some mathematical insight on the origin of such slow process has been proposed: it has been argued that the dissipation rate may become arbitrarily small in certain physical regimes due to the decoupling of non-resonant terms, as it happens in KAM problems [37, 38].

A renewed interest in the problem of boundary cooling was provided by the proposal of implementing it as a technique to localize Bose-Einstein condensates in optical lattices [39]. Referring to the DNLS model, stationary and

traveling localized states were generated by removing atoms at the optical-lattice ends. Regimes of stretched-exponential decay for the number of atoms trapped in the lattice were clearly identified by numerical simulations. Further studies showed that the dynamics of dissipated energy exhibits a characteristic avalanche behavior [40].

4.2 Dynamical freezing of relaxation to equilibrium

In this Section we discuss the relaxation process of a localized excitation (DB) in the DNLS model (see Eqs. (4-5)). For positive temperatures, DBs have a negligible probability to arise at equilibrium and yet, as commented above, there are ways to grow them (e.g., by boundary dissipation). Therefore, it is important to understand their relaxation process.

Simulations have been performed by superposing a large-mass DB at the origin, $n = 0$, to an otherwise equilibrium configuration for the background (i.e. $-N \leq n \leq N$). The temperature $T = 10$ and the chemical potential $\mu = -6.4$ are imposed by connecting the chain boundaries to suitable Langevin baths.

The main results are reported in Fig. 1, where we can see the time dependence of the breather mass $b = |z_0|^2$ in a typical simulation (notice the logarithmic time scale). The decay process is fairly abrupt and we can identify quasi-stationary regimes, separated by jumps. Because of the abrupt decay of $b(t)$ we can define the relaxation time τ_b by setting a threshold b^* (dashed horizontal line). In the inset, we show how τ_b depends on the initial mass of the breather, namely exponentially. In the rest of this Section we will discuss the meaning of this numerical finding and some related results.

The rapid increase of τ_b with $b(0)$ suggests that the larger the mass of the breather, the weaker the relaxation mechanism. This is not surprising, because the natural frequency of a breather of mass b is $\omega = 2b$, so the coupling term between the breather and the nearest neighbors becomes negligible on the typical time scale of the background (which is of order one). However, a rotational frequency proportional to the breather mass cannot justify by itself an exponentially slow decay process. Before trying any theoretical explanation, it is necessary to gain more insight on the relaxation process.

From Fig. 1 we can see that the *laminar* regime preceding the final breather disruption is approximately quasi-stationary, with no specific drift (except for the final part, where the mass clearly tends to decrease). It is, therefore, tempting to characterize this regime in terms of a suitable diffusion coefficient². The next question is the identification of an optimal variable to characterize the hypothetical diffusion process. The mass $b(t)$ is too noisy to extract reliable estimates. A principal component analysis (PCA) performed

² Bounded fluctuations would be possible only in the presence of an attractor, but this is a Hamiltonian system.

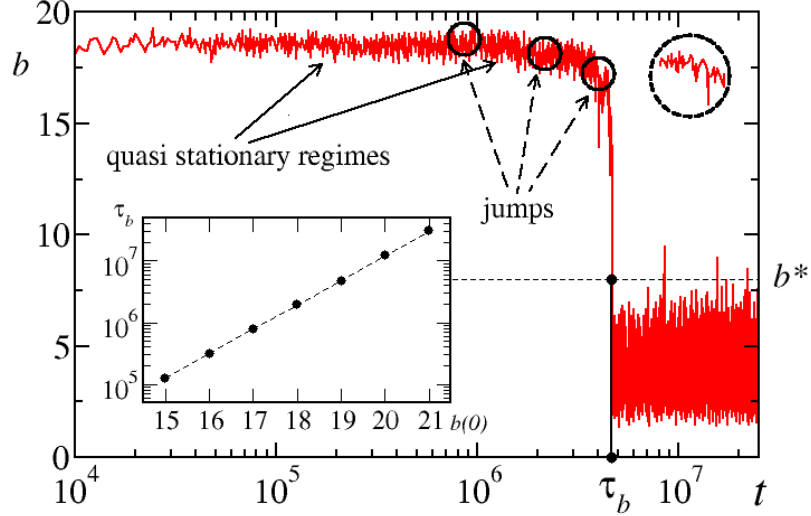


Fig. 1 The relaxation process of a breather through the time dependence of its mass, $b(t)$. The abrupt character of the process allows to define a threshold value b^* and to determine the relaxation time τ_b as the shortest time satisfying the condition $b(\tau_b) = b^*$. In the top right circle we zoom in a jump of the mass. The inset shows the exponential increase of τ_b with the initial mass of the breather: the dashed line is a fit, giving $\tau_b \approx e^{\alpha b(0)}$, with $\alpha = 0.91 \pm 0.01$. The breather is initially at the centre of a chain of $N = 31$ sites.

on the triplet of variables z_{-1}, z_0, z_1 suggests to use $\tilde{Q} \simeq E_b^{1/4}$ [41], where $E_b = |z_0|^4 + \frac{1}{2}[z_0^*(z_1 + z_{-1}) + \text{c.c.}]$ is the breather energy (see Eq. (4)). Accordingly we define $D_{\tilde{Q}} = \langle [\tilde{Q}^2(t + \tau) - \tilde{Q}^2(t)] \rangle / \tau$. The evaluation of $D_{\tilde{Q}}$ for breathers of increasing height (see Fig. 4 of Ref. [41]) shows that the diffusion coefficient decreases exponentially with $b(0)$, in agreement with the direct evidence of an almost frozen dynamics. On the basis of fluctuation-dissipation considerations, we should also expect a drift $v \approx D_{\tilde{Q}}/T$ and, accordingly, an exponential increase of the decay time. However, while the exponential increase is confirmed by the simulations, we do not see a clear evidence of a (downward) drift.

Fig. 1 rather suggests that the relaxation is accompanied and perhaps caused by sporadic jumps. This statement is supported by Fig. 2, where we plot the average transfer of energy between the breather and the background in a given interval of time, as a function of the initial mass of the neighbouring site, $a_1(0)$ (suitably rescaled). There is an evident, narrow peak accompanied by some pinnacles. The peak appears at a value very close to the analytical

threshold for the existence of symmetric bound states (dimers) between two neighbouring sites, $\sqrt{a_1^*(0)} = \sqrt{b(0)} - \sqrt{2}$.

The very emergence of such bound states is attested by the inset of the same figure, where we plot the time dependence of the mass of the breather $b(t)$ along with the mass $a_1(t)$ of a neighboring site. When it happens that $a_1 > a_1^*$ (see the dashed line) the two sites are strongly coupled together and rotate with the same frequency. This bound state eventually dissolves, with the net result that the “post-dimer” breather has lost some energy with respect to the “pre-dimer” one.

Analytical, non-rigorous considerations allow evaluating the typical time scale of such phenomena as the expectation time for a background fluctuation in one of the two neighbouring sites to become larger than the threshold a_1^* . In fact, from the high- T equilibrium distribution $P(\theta)$ to have a mass θ [23], we can approximately estimate the breather lifetime $\tau_b \approx 1/P(a_1^*)$, which has the asymptotic expression $\tau_b \approx \exp(\beta b^2)$ for a diverging breather mass b . This expression implies a superexponential growth of the relaxation time with the mass, suggesting that the asymptotic mechanism for breather decay might not be dimer formation (τ_b seems to increase exponentially), but current simulation data do not allow to exclude it either.

As a matter of fact, the additional peaks appearing in Fig. 2 suggest the existence of other mechanisms and the special setup we are going to discuss allows one to conclude that relaxation occurs even if dimer formation is suppressed. We direct reader’s attention to the inset of Fig. 3, where we consider the relaxation process of the very same breather in different conditions. The full line is the standard DNLS model, i.e. a curve fully similar to that plotted in Fig. 1. The dotted line has been determined with a unidirectional coupling between breather and background: the former feels the latter but not the other way around. In practice the breather is coupled to a background whose evolution is independent of the breather itself. The result is a qualitatively similar evolution of the breather mass.

Since unidirectional coupling makes impossible the rising of a symmetric bound state, in this case dimers cannot play any role in DB relaxation. On the other hand, resonance mechanisms would not be affected by the unidirectional character of the coupling and therefore they would persist, but the approximate expression for the relaxation time would still give a superexponential growth.

Unidirectional coupling is useful also to discuss the temperature dependence of the relaxation time, $\tau_b(T)$. The curves plotted in Fig. 3 refer to different initial masses of the breather and the central result we focus on is the asymptotic behavior of $\tau_b(T)$, which seems to reach a constant. In other words, the relaxation time of a finite breather is expected to be finite even at infinite temperature. The horizontal lines have been determined analytically with the same criterion discussed here above, taking the limit $T \rightarrow \infty$ but also allowing $|\mu| = T/a$ to diverge so that the density of mass, a , is kept constant (simulations have been performed within such setup).

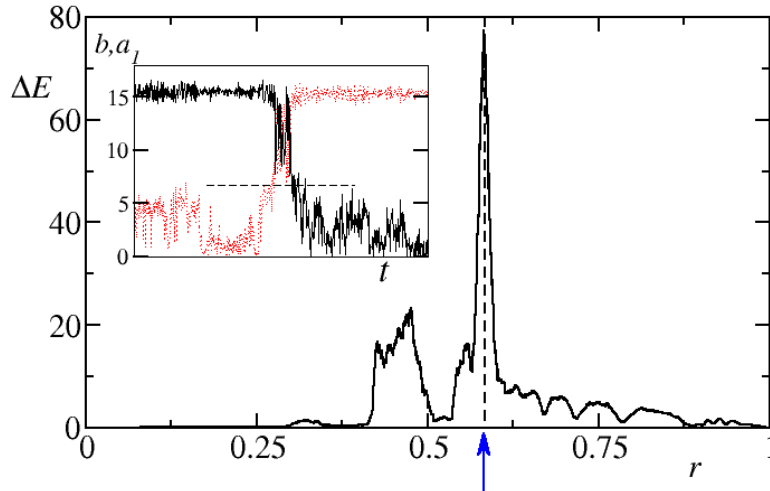


Fig. 2 The energy lost or gained on average by the breather after a fixed amount of time, as a function of the initial mass of the neighbouring site, $a_1(0)$ (more precisely, of the ratio $r = a_1(0)/b(0)$). The sharp peak corresponds to the condition $\sqrt{a_1(0)} = \sqrt{b(0)} - \sqrt{2}$, which allows the formation of a symmetric bound state (dimer) between the breather and its neighbour. In the inset we plot the time dependence of the mass in these two sites along with such threshold value (horizontal dashed line).

So far, we have mentioned two potentially interesting processes: (i) the diffusion occurring during the laminar (quasi-stationary) regime; (ii) the jumps, both visible in Fig. 1. The diffusion coefficient turns out to decrease exponentially with b and the probability of dimer or resonances formation (related to the jumps) also decreases exponentially or even superexponentially. It is evident that in the presence of several relaxation channels, a frozen dynamics may appear if and only if all mechanisms are exponentially slow.

However, it is not clear at all *why* dynamics is almost frozen. A former paper by some of the present authors [41] - a first attempt in this direction - suggests that \tilde{Q} (the quantity derived from the PCA analysis and used to derive the diffusion coefficient) is the approximate expression of an Adiabatic Invariant (AI), which might be broken by jumps. We have tried to determine AI perturbatively, by computing higher orders, but the attempt has not been successful.

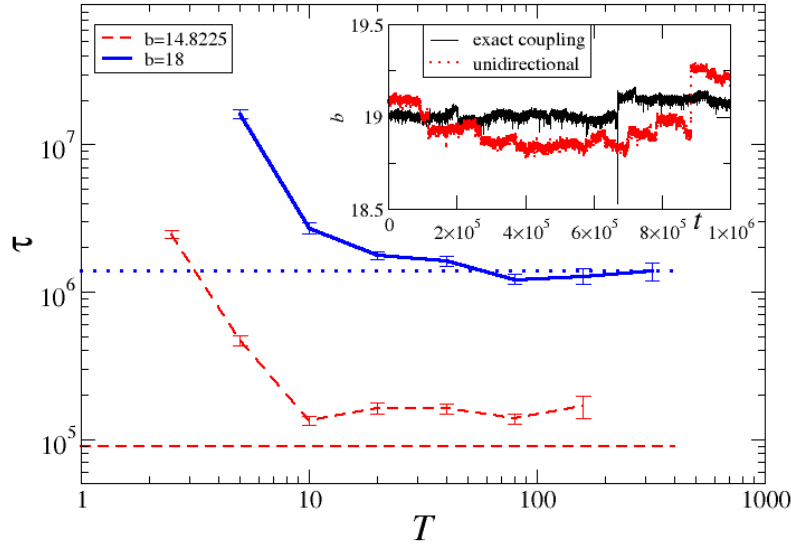


Fig. 3 The relaxation time of a breather as a function of the temperature T , for two different initial masses. The horizontal lines represent the analytical, asymptotic values as deduced by an approximate approach (see the main text) where the breather feels the background but not the other way around. In the inset we compare the time evolution of the mass of the same initial breather, with exact and unidirectional coupling.

We wish to stress that understanding the relaxation process of a breather at positive temperature is a useful if not necessary step to later understand the negative T phase from a dynamical point of view.

4.3 Role of negative temperatures

In the previous section we have seen that relaxation to equilibrium may be very slow in the DNLS, in the positive temperature region of the (a, h) plane. As mentioned in Section 3, there exists a second region ($h > 2a^2$) where the absolute temperature is expected to be negative (on the basis of microcanonical arguments). Relaxation phenomena in this region turn out to be a rather controversial issue, not yet fully settled.

Entropic arguments [42, 43] suggest that all the excess energy, which cannot be stored in a homogeneous background for $h > 2a^2$, should eventually concentrate into a single breather. In fact, this is precisely what happens in

a simplified, purely stochastic version of the DNLS, where it has been shown that multiple breathers progressively merge through a non conventional coarsening process [44, 45].

On the other hand, coalescence has not been observed in molecular dynamics simulations slightly above the $\beta = 0$ line (e.g. for $a = 1$ and $h = 2.4$). On the contrary, it looks like a sort of stationary regime sets in, characterized by a small breather density, where DBs spontaneously form and then die, after some typical lifetime [24], see Fig. 4. This is due to the presence of a finite interaction (hopping) energy: the background can store excess energy in the phase differences of neighbouring sites and this implies that breathers can spontaneously nucleate. These findings have been recently confirmed by more extensive simulations [46] which suggest the existence of a finite region in the (a, h) -plane, where the dynamics covers a subregion of the available phase space, doing so in an “ergodic manner” (i.e. no coarsening).

Further, independent evidence of a relatively stable negative-temperature regime comes from the nonequilibrium simulations performed in [47], where a DNLS chain was put in contact on one side with a positive temperature heat bath, while on the other, with a pure dissipator. Depending on the temperature value of the first heat bath, an extended portion of the chain, settles in a regime characterized by a position-dependent negative temperature, a flux of mass and energy, without being accompanied by the onset of breathers.

Finally, recent statistical-mechanics calculations [25] suggest that slightly above the critical $\beta = 0$ line, strong finite-size effects are to be expected, which might affect the interpretation of the numerical simulations.

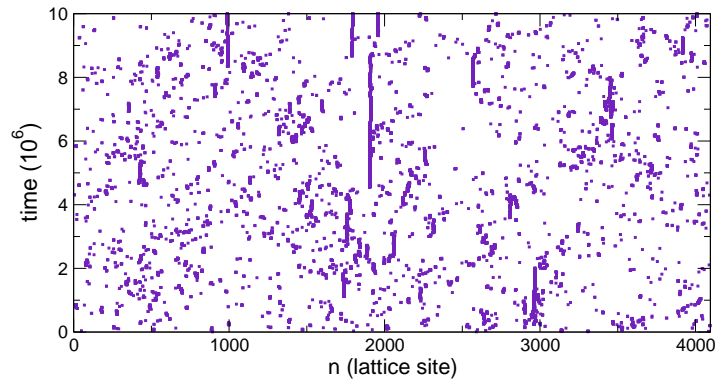


Fig. 4 Evolution of the local amplitude for DNLS in a negative temperature state, the dots correspond to points where $|z_n|^2 > 10$. Microcanonical simulation with $a = 1$ and $h = 2.4$, $N = 4192$.

5 Transport

Let us now turn our attention to nonequilibrium steady states that emerge, at long enough times, when the system is in contact with two (or more) heat reservoirs operating at different temperatures. Generally speaking, several methods, based on both deterministic and stochastic (Langevin or Monte-Carlo) algorithms, have been proposed [28]. A complementary approach is based on linear-response theory, which amounts to computing the equilibrium correlation function of currents. In principle, this task can be accomplished in any equilibrium ensemble, the microcanonical one being the most natural choice.

5.1 Anomalous energy transport

The main results, emerging from a long series of works, can be summarized as follows. Models of the form (2) with $U(q) = 0$ typically display *anomalous* transport and relaxation features. Said differently, Fourier's law *does not hold*: the kinetics of energy carriers is so correlated that they are able to propagate *faster* than in the standard (diffusive) case. We refer the reader to existing review papers [28, 48, 49, 1] for a more comprehensive description. Here we just mention how this anomalous behaviour manifests itself in the simulations.

- The finite-size heat conductivity $\kappa(L)$ diverges in the limit of a large system size $L \rightarrow \infty$ as $\kappa(L) \propto L^\gamma$ [50], i.e. the heat transport coefficient is ill-defined in the thermodynamic limit.
- The equilibrium correlation function of the total energy current J displays a nonintegrable long-time tail $\langle J(t)J(0) \rangle \propto t^{-(1-\delta)}$, with $0 \leq \delta < 1$ [51, 52]. Accordingly, the Green-Kubo formula yields an infinite value of the conductivity.
- Energy perturbations propagate superdiffusively [53, 54]: a local perturbation of the energy spreads, while its variance broadens in time as $\sigma^2 \propto t^\beta$, with $\beta > 1$.
- Temperature profiles in the nonequilibrium steady states are nonlinear, even for vanishing applied temperature gradients. Typically they are the solution of a *fractional heat equation* [55, 56].

There is a large body of numerical evidence that the above features occur generically in 1D and 2D, whenever the conservation of energy, momentum and length holds. This is related to the existence of long-wavelength (Goldstone) modes (an acoustic phonon branch in the linear spectrum of (2) with $U = 0$) that are very weakly damped. Indeed, it is sufficient to add external (e.g. substrate) forces, to make all anomalies disappear and restore Fourier's law.

5.2 Universality and the Kardar-Parisi-Zhang equation

The nonlinear fluctuating hydrodynamics approach is able to justify and predict several universal features of anomalous transport in anharmonic chains [22, 57]. The main entities are the random fields describing deviations of the conserved quantities with respect to their stationary values. The role of fluctuations is taken into account by renormalization group or some kind of self-consistent theory.

The main theoretical insight is the intimate relation between the anharmonic chain and one of the most important equations in nonequilibrium statistical physics, the celebrated Kardar-Parisi-Zhang (KPZ) equation, originally introduced in the (seemingly unrelated) context of surface growth [58]. The KPZ equation for the stochastic field $h(x, t)$ in one spatial dimension reads

$$\frac{\partial h}{\partial t} = \nu \frac{\partial^2 h}{\partial x^2} + \frac{\kappa}{2} \left(\frac{\partial h}{\partial x} \right)^2 + \eta. \quad (7)$$

where $\eta(x, t)$ represents a Gaussian white noise with $\langle \eta(x, t) \eta(x', t') \rangle = 2D \delta(x - x') \delta(t - t')$ and ν, κ, D are the relevant parameters. It has been shown [22, 57] that large-scale dynamical properties of anharmonic chains are in the same dynamical universality class as Eq.(7). Loosely speaking, we can represent the displacement field as the superposition of counter-propagating plane waves, modulated by an envelope that is ruled, at large scales, by Eq. (7). As a consequence, correlations of observables display in the hydrodynamic limit *anomalous dynamical scaling*. For instance, the dynamical structure factor $S(k, \omega)$ of the particle displacement shows for $k \rightarrow 0$ two sharp peaks at $\omega = \pm \omega_{\max}(k)$ that correspond to the propagation of sound modes and for $\omega \approx \pm \omega_{\max}$ behave as

$$S(k, \omega) \sim f_{\text{KPZ}} \left(\frac{\omega \pm \omega_{\max}}{\lambda_s k^{3/2}} \right). \quad (8)$$

Remarkably, the scaling function f_{KPZ} is universal and known exactly, while λ_s is a model-dependent parameter. The main point is that the *dynamical exponent* $z = 3/2$ is different from $z = 2$ expected for a standard diffusive process.

Most of the predictions have been successfully tested for several models. For a chain of coupled anharmonic oscillators with three conserved quantities like the FPUT chains, such theoretical predictions have been successfully compared with the numerics [59, 60]. Other positive tests have been reported in Ref. [61]. One further prediction is that the FPUT- β model should belong to a different (non-KPZ) universality class, as previously suggested by the numerics [62, 63].

5.3 Coupled transport

As known from irreversible thermodynamics, when there are more conserved quantities, the corresponding currents can be coupled: in the linear response regime, transport is described by Onsager coefficients. The best-known example is that of thermoelectricity, whereby useful electric work can be extracted in the presence of temperature gradients [64, 65, 66].

In the present context, the simplest example is the one-dimensional rotor model, Eq. (6), that admits two conserved quantities (energy and angular momentum), two associated currents, and only one relevant thermodynamic parameter, the temperature T . In this case [44] one can easily introduce the interaction with two reservoirs by fixing the average angular momenta ω_0, ω_1 and kinetic temperatures T_0, T_1 at the chain ends. This can be obtained by adding the Langevin term $\gamma(\omega_0 - \dot{q}_1) + \sqrt{2\gamma T_0} \xi$ to the equation of motion (6) of the leftmost rotor: γ defines the coupling strength with the bath and ξ is a Gaussian white random noise with zero mean and unit variance. An analogous term, with ω_1 and T_1 replacing ω_0 and T_0 , is added to the equation of motion of the rightmost rotor.

To illustrate the peculiarities of this setup, Fig. 5 reports frequency and temperature profiles [67] in a case where only an angular momentum gradient is applied, i.e. $T_1 = T_0$ and $\omega_0 = -1$ and $\omega_1 = 1$. The temperature profile T_n is non-monotonic [68] as a consequence of the coupling with the momentum flux j_p imposed by the torque at the boundaries, although, in the end, the energy flux j_h vanishes for symmetry reasons. By recalling that $j_h = j_q + \omega j_p$ we see that the heat flux $j_q = -\omega j_p$ varies along the chain being everywhere proportional to the frequency, so that it is negative in the left part and positive in the right side (this is again consistent with symmetry considerations). Thus heat is generated in the central hotter region, where the temperature is higher and transported towards the two edges. The total energy flux is however everywhere zero as the heat flux is compensated by an opposite coherent flux due to momentum transfer. Physically, the temperature bump can be interpreted as a sort of Joule effect: the transport of momentum involves dissipation, which in turn contributes to increasing the temperature, analogously to what happens when an electric wire is crossed by a flux of charges.

Similar effects are studied in [27] for the DNLS case, where the dependence of the Onsager matrix on temperature and chemical potential is considered. In this case the cross-coupling term (the equivalent of the Seebeck coefficient in the language of thermo-electricity) may change sign, leading to temperature- and mass-profiles with opposite slopes.

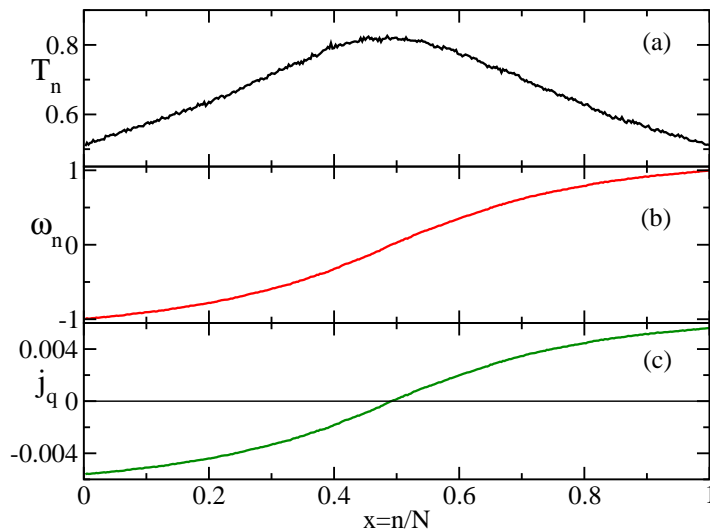


Fig. 5 Simulation of the rotor chain with $N = 400$ particles, in contact at its boundaries with two heat baths at temperature $T_0 = T_1 = 0.5$ and in the presence of torques $\omega_0 = -1$ and $\omega_1 = 1$: (a) temperature profile; (b) frequency (chemical potential) profile; (c) local heat flux.

5.4 Integrable models and their perturbations

The above results are mostly obtained in a strongly nonlinear regime or more generally far from any integrable limit. For the FPUT model, this means working with high enough energies/temperatures to avoid all the difficulties induced by quasi-integrability and the associated slow relaxation to equilibrium.

Integrable systems constitute *per se* a relevant case. In the framework of the present work the most important example is certainly the celebrated Toda chain, namely model (1) with $U = 0$ and

$$V(x) = e^{-x} + x - 1$$

As intuitively expected, heat transport is ballistic due to its integrability and the associated solitonic solution [69]. Mathematically, this is expressed by saying that there is a non-vanishing *Drude weight*, namely a zero-frequency component of the energy current power spectra [70, 71]. A lower bound of the Drude weight can be estimated making use of Mazur inequality [72] in terms of correlations between the currents themselves and the conserved quantities (see [70, 71] for the Toda case). However, the idea of solitons transporting energy as independent particles is somehow too simplistic. It has been recognized [73] that solitons experience a stochastic sequence of spatial shifts as they move through the lattice interacting with other excitations without

momentum exchange [73]. At variance with the harmonic chain, which is also integrable, but whose proper modes are non-interacting phonons, the Toda chain, as proposed in [74], is an interacting integrable system. In particular, it is characterized by what has been termed a non-dissipative diffusion mechanism [73]. In fact, the calculation of the transport coefficients by the Green-Kubo formula indicates the presence of a finite Onsager coefficient, which corresponds to a diffusive process on top of the dominant ballistic one [71, 75, 76].

A natural question concerns the behavior when a generic perturbation is applied to an otherwise integrable system. For instance, adding a quadratic pinning potential $U(q) = q^2/2$ to the Toda chain is expected to restore standard diffusive transport, but numerical simulations show that long-range correlations are preserved over relatively long scales [76, 77]. Moreover, weak perturbations that conserve momentum (and are thus expected to display anomalous transport in the KPZ class) display instead significant differences [78] and even diffusive transport over the accessible simulation ranges [79]. Altogether a full unified picture of the problem is still lacking.

6 Overview and open problems

In spite of the sensible progress that has been made over the last decades, the study of nonequilibrium processes in nonlinear systems remains a fascinating and challenging domain of research. On a methodological ground, it concerns mainly the scientific communities of mathematics and theoretical physics, but it is of primary interest also for optics, materials science and soft matter, just to mention a few among the related fields in experimental and applied research. Going through the reading of this Chapter, one can easily realize that most achievements have been possible thanks to a fruitful combination of analytic approaches and numerical simulations and this can be reasonably expected to hold also in the future. For what concerns open problems, it is worth mentioning a few of them, that have already attracted some interest. The first one is the study of nonlinear models with long-range interactions. The main motivation stems from the observation that for this class of models the equivalence between statistical ensembles may not hold. This is expected to yield interesting consequences also for nonequilibrium phenomena. In fact, long-range systems are known to exhibit further peculiar properties, like long-living metastable states, anomalous energy diffusion, lack of thermalization when interacting with a single temperature reservoir, propagation of perturbations with infinite velocity, etc. (for a general review see [80]). The problem of heat transport in the long-range version of the rotor and FPUT chains has been recently tackled in a series of papers [81, 82, 83, 84, 85]. When the interaction is genuinely long-range, i.e. the long-range exponent α is smaller than 1, the heat transport process is domi-

nated by parallel transport: a flat temperature profile sets in, simply because each oscillator, independently, takes a temperature value which is the average of those applied by the thermal baths. For α larger than 1, the long-range rotor model reproduces standard diffusion, i.e. normal heat conductivity, as in the short-range version. Conversely, the FPUT chain is characterized by an anomalous scaling exponent $\gamma(\alpha)$, which seems to recover the value of the short-range case only for large values of α . Anyway, a better understanding of the transport problem demands further refined investigations, that should take into account also a comparison with the unusual relaxation process to equilibrium characterizing long-range systems.

Let us conclude by mentioning one further open problem, which is related to energy localization induced by nonlinearity. In fact, localization processes may emerge in nonlinear systems even in the absence of disorder. The typical example is the spontaneous formation of breathers in the DNLS problem already discussed in Section 4. In the negative temperature region the phenomenon of condensation of DBs can be read as a process of ergodicity-breaking, because, in the microcanonical setup, energy equipartition is inhibited by its localization. It is well known that, when condensation phenomena are present, statistical ensemble equivalence is not granted [86]. This is the case of the DNLS Hamiltonian in the negative temperature region, where the only available statistical ensemble is the microcanonical one [25]. It is worth recalling that both total energy and mass are conserved quantities in the DNLS Hamiltonian: the breaking of ergodicity in the negative temperature phase indicates that a standard thermalization process for both quantities is suppressed. The analogy with the problem of the Eigenvalue Thermalization Hypothesis advanced for genuine quantum integrable systems (see the review paper [87]) suggests that ensemble equivalence should be reconsidered also in this context to properly formulate a thermalization hypothesis or, alternatively, the many-body localization phenomenon invoked in quantum integrable systems.

References

1. Stefano Lepri, editor. *Thermal transport in low dimensions: from statistical physics to nanoscale heat transfer*, volume 921 of *Lect. Notes Phys.* Springer-Verlag, Berlin Heidelberg, 2016.
2. Roberto Livi and Paolo Politi. *Nonequilibrium statistical physics: a modern perspective*. Cambridge University Press, 2017.
3. MJ Gillan and RW Holloway. Transport in the Frenkel-Kontorova model 3: thermal conductivity. *J. Phys. C*, 18(30):5705–5720, 1985.
4. Bambi Hu, Baowen Li, and Hong Zhao. Heat conduction in one-dimensional chains. *Phys. Rev. E*, 57(3):2992, 1998.
5. K. Aoki and D. Kusnezov. Bulk properties of anharmonic chains in strong thermal gradients: non-equilibrium ϕ^4 theory. *Phys. Lett. A*, 265(4):250, 2000.
6. Panayotis G Kevrekidis and Jesus Cuevas-Maraver. *A Dynamical Perspective on the ϕ^4 Model: Past, Present and Future*, volume 26. Springer, 2019.

7. Giulio Casati, Joseph Ford, Franco Vivaldi, and William M. Visscher. One-dimensional classical many-body system having a normal thermal conductivity. *Phys. Rev. Lett.*, 52(21):1861–1864, 1984.
8. Enrico Fermi, J Pasta, and S Ulam. Studies of nonlinear problems. *Los Alamos Report LA-1940*, page 978, 1955.
9. DN Payton, M Rich, and WM Visscher. Lattice thermal conductivity in disordered harmonic and anharmonic crystal models. *Phys. Rev.*, 160(3):706–&, 1967.
10. Hiroshi Nakazawa. On the lattice thermal conduction. *Progress of Theoretical Physics Supplement*, 45:231–262, 1970.
11. H Kaburaki and M Machida. Thermal-conductivity in one-dimensional lattices of Fermi-Pasta-Ulam type. *Phys. Lett. A*, 181(1):85–90, SEP 27 1993.
12. J. C. Eilbeck, P. S. Lomdahl, and A. C. Scott. The discrete self-trapping equation. *Physica D*, 16:318338, 1985.
13. J. C. Eilbeck and M. Johansson. The discrete nonlinear Schroedinger equation-20 years on. In L. Vazquez, R. S. MacKay, and M. P. Zorzano, editors, *Conference on Localization and Energy Transfer in Nonlinear Systems*, page 44. World Scientific, Singapore, 2003.
14. Panayotis G. Kevrekidis. *The Discrete Nonlinear Schrödinger Equation*. Springer Verlag, Berlin, 2009.
15. A. Scott. *Nonlinear science. Emergence and dynamics of coherent structures*. Oxford University Press, Oxford, 2003.
16. A. M. Kosevich and M. A. Mamalui. Linear and nonlinear vibrations and waves in optical or acoustic superlattices (photonic or phonon crystals). *J. Exp. Theor. Phys.*, 95(4):777, 2002.
17. D. Hennig and G.P. Tsironis. Wave transmission in nonlinear lattices. *Phys. Rep.*, 307(5-6):333432, 1999.
18. R. Franzosi, R. Livi, G.L. Oppo, and A. Politi. Discrete breathers in BoseEinstein condensates. *Nonlinearity*, 24:R89, 2011.
19. Sergej Flach and Andrey V Gorbach. Discrete breathers – advances in theory and applications. *Phys. Rep.*, 467(1):1–116, 2008.
20. Magnus Johansson and Kim Rasmussen. Statistical mechanics of general discrete nonlinear Schroedinger models: Localization transition and its relevance for Klein-Gordon lattices. *Physical Review E*, 70(6):066610, 2004.
21. S Iubini, S Lepri, R Livi, and A Politi. Off-equilibrium Langevin dynamics of the discrete nonlinear Schroedinger chain. *J. Stat. Mech: Theory Exp.*, (08):P08017, 2013.
22. Herbert Spohn. Nonlinear fluctuating hydrodynamics for anharmonic chains. *J. Stat. Phys.*, 154(5):1191–1227, 2014.
23. K Rasmussen, T. Cretigny, Panayotis G. Kevrekidis, and N. Grnbech-Jensen. Statistical mechanics of a discrete nonlinear system. *Phys. Rev. Lett.*, 84(17):37403743, 2000.
24. S Iubini, R Franzosi, R Livi, GL Oppo, and A Politi. Discrete breathers and negative-temperature states. *New J. Phys.*, 15(2):023032, 2013.
25. Giacomo Gradenigo, Stefano Iubini, Roberto Livi, and Satya N. Majumdar. Localization in the discrete non-linear Schroedinger equation: mechanism of a first-order transition in the microcanonical ensemble, 2019. arXiv:1910.07461.
26. Hans Henrik Rugh. Dynamical approach to temperature. *Phys. Rev. Lett.*, 78(5):772, 1997.
27. S. Iubini, S. Lepri, and A. Politi. Nonequilibrium discrete nonlinear Schroedinger equation. *Phys. Rev. E*, 86(1):011108, 2012.
28. S Lepri, R Livi, and A Politi. Thermal conduction in classical low-dimensional lattices. *Phys. Rep.*, 377:1, 2003.
29. Haruo Yoshida. Construction of higher order symplectic integrators. *Phys. Lett. A*, 150(5-7):262–268, 1990.

30. G. Benettin and A. Poincaré. Time-scales to equipartition in the Fermi–Pasta–Ulam problem: Finite-size effects and thermodynamic limit. *Journal of Statistical Physics*, 144(4):793, Aug 2011.
31. G. Benettin, H. Christodoulidi, and A. Poincaré. The Fermi-Pasta-Ulam problem and its underlying integrable dynamics. *Journal of Statistical Physics*, 152(2):195–212, Jul 2013.
32. Miguel Onorato, Lara Vozella, Davide Proment, and Yuri V. Lvov. Route to thermalization in the α -Fermi-Pasta-Ulam system. *Proceedings of the National Academy of Sciences*, 112(14):4208–4213, 2015.
33. GP Tsironis and S Aubry. Slow relaxation phenomena induced by breathers in nonlinear lattices. *Phys. Rev. Lett.*, 77(26):5225, 1996.
34. F Piazza, S Lepri, and R Livi. Slow energy relaxation and localization in 1d lattices. *J. Phys. A: Math. Gen.*, 34(46):9803, 2001.
35. Francesco Piazza, Stefano Lepri, and Roberto Livi. Cooling nonlinear lattices toward energy localization. *Chaos: An Interdisciplinary Journal of Nonlinear Science*, 13(2):637–645, 2003.
36. Maria Eleftheriou, Stefano Lepri, Roberto Livi, and Francesco Piazza. Stretched-exponential relaxation in arrays of coupled rotators. *Physica D: Nonlinear Phenomena*, 204(3):230–239, 2005.
37. Noe Cuneo and J-P Eckmann. Non-equilibrium steady states for chains of four rotors. *Communications in Mathematical Physics*, 345(1):185–221, 2016.
38. Noe Cuneo, Jean-Pierre Eckmann, and C Eugene Wayne. Energy dissipation in hamiltonian chains of rotators. *Nonlinearity*, 30(11):R81–R117, oct 2017.
39. Roberto Livi, Roberto Franzosi, and Gian-Luca Oppo. Self-localization of Bose-Einstein condensates in optical lattices via boundary dissipation. *Phys. Rev. Lett.*, 97:60401, 2006.
40. GS Ng, Holger Hennig, Ragnar Fleischmann, Tsampikos Kottos, and Theo Geisel. Avalanches of Bose–Einstein condensates in leaking optical lattices. *New journal of physics*, 11(7):073045, 2009.
41. Stefano Iubini, Liviu Chirondojan, Gian-Luca Oppo, Antonio Politi, and Paolo Politi. Dynamical freezing of relaxation to equilibrium. *Phys. Rev. Lett.*, 122:084102, Mar 2019.
42. Benno Rumpf. Simple statistical explanation for the localization of energy in nonlinear lattices with two conserved quantities. *Phys. Rev. E*, 69(1):016618, 2004.
43. Benno Rumpf. Transition behavior of the discrete nonlinear Schroedinger equation. *Phys. Rev. E*, 77(3):036606, 2008.
44. Stefano Iubini, Stefano Lepri, Roberto Livi, and Antonio Politi. Boundary-induced instabilities in coupled oscillators. *Phys. Rev. Lett.*, 112:134101, 2014.
45. Stefano Iubini, Antonio Politi, and Paolo Politi. Relaxation and coarsening of weakly-interacting breathers in a simplified DNLS chain. *Journal of Statistical Mechanics: Theory and Experiment*, 2017(7):073201, jul 2017.
46. Thudiyangal Mithun, Yagmur Kati, Carlo Danieli, and Sergej Flach. Weakly nonergodic dynamics in the Gross-Pitaevskii lattice. *Physical review letters*, 120(18):184101, 2018.
47. Stefano Iubini, Stefano Lepri, Roberto Livi, Gian-Luca Oppo, and Antonio Politi. A chain, a bath, a sink, and a wall. *Entropy*, 19(9), 2017.
48. Abhishek Dhar. Heat transport in low-dimensional systems. *Adv. Phys.*, 57:457–537, 2008.
49. G. Basile, L. Delfino, S. Lepri, R. Livi, S. Olla, and A. Politi. Anomalous transport and relaxation in classical one-dimensional models. *Eur. Phys. J.-Special Topics*, 151:85–93, 2007.
50. S Lepri, R Livi, and A Politi. Heat conduction in chains of nonlinear oscillators. *Phys. Rev. Lett.*, 78(10):1896–1899, MAR 10 1997.
51. S Lepri, R Livi, and A Politi. On the anomalous thermal conductivity of one-dimensional lattices. *Europhys. Lett.*, 43(3):271–276, AUG 1 1998.

52. S Lepri. Memory effects and heat transport in one-dimensional insulators. *Eur. Phys J. B*, 18(3):441–446, DEC 2000.
53. S. Denisov, J. Klafter, and M. Urbakh. Dynamical heat channels. *Phys. Rev. Lett.*, 91(19):194301, 2003.
54. P. Cipriani, S. Denisov, and A. Politi. From anomalous energy diffusion to Levy walks and heat conductivity in one-dimensional systems. *Phys. Rev. Lett.*, 94(24):244301, 2005.
55. Stefano Lepri and Antonio Politi. Density profiles in open superdiffusive systems. *Phys. Rev. E*, 83(3):030107, 2011.
56. Aritra Kundu, Cedric Bernardin, Keji Saito, Anupam Kundu, and Abhishek Dhar. Fractional equation description of an open anomalous heat conduction set-up. *J. Stat. Mech.: Theory Exp.*, 2019(1):013205, 2019.
57. Henk van Beijeren. Exact results for anomalous transport in one-dimensional hamiltonian systems. *Phys. Rev. Lett.*, 108:180601, 2012.
58. A-L Barabasi and H E Stanley. *Fractal concepts in surface growth*. Cambridge university press, 1995.
59. Suman G Das, Abhishek Dhar, Keiji Saito, Christian B Mendl, and Herbert Spohn. Numerical test of hydrodynamic fluctuation theory in the Fermi-Pasta-Ulam chain. *Phys. Rev. E*, 90(1):012124, 2014.
60. Pierfrancesco Di Cintio, Roberto Livi, Hugo Bufferand, Guido Ciraolo, Stefano Lepri, and Mika J. Straka. Anomalous dynamical scaling in anharmonic chains and plasma models with multiparticle collisions. *Phys. Rev. E*, 92:062108, 2015.
61. Christian B. Mendl and Herbert Spohn. Dynamic correlators of Fermi-Pasta-Ulam chains and nonlinear fluctuating hydrodynamics. *Phys. Rev. Lett.*, 111:230601, 2013.
62. S Lepri, R Livi, and A Politi. Universality of anomalous one-dimensional heat conductivity. *Phys. Rev. E*, 68(6, Part 2):067102, DEC 2003.
63. GR Lee-Dadswell. Universality classes for thermal transport in one-dimensional oscillator systems. *Phys. Rev. E*, 91(3):032102, 2015.
64. C. Mejia-Monasterio, H. Larralde, and F. Leyvraz. Coupled normal heat and matter transport in a simple model system. *Phys. Rev. Lett.*, 86(24):5417–5420, 2001.
65. Giulio Casati, Lei Wang, and Tomaz Prosen. A one-dimensional hard-point gas and thermoelectric efficiency. *J. Stat. Mech.: Theory and Experiment*, (03):L03004, 2009.
66. Giuliano Benenti, Giulio Casati, and Carlos Mejia-Monasterio. Thermoelectric efficiency in momentum-conserving systems. *New J. Phys.*, 16(1):015014, 2014.
67. S Iubini, S Lepri, R Livi, and A Politi. Coupled transport in rotor models. *New J. Phys.*, 18(8):083023, 2016.
68. A. Iacobucci, F. Legoll, S. Olla, and G. Stoltz. Negative thermal conductivity of chains of rotors with mechanical forcing. *Phys. Rev. E*, 84(6):061108, 2011.
69. M Toda. Solitons and heat-conduction. *Phys. Scr.*, 20(3-4):424–430, 1979.
70. X Zotos. Ballistic transport in classical and quantum integrable systems. *J. Low. Temp. Phys.*, 126(3-4):1185–1194, 2002.
71. B Sriram Shastry and AP Young. Dynamics of energy transport in a Toda ring. *Phys. Rev. B*, 82(10):104306, 2010.
72. P Mazur. Non-ergodicity of phase functions in certain systems. *Physica*, 43(4):533–545, 1969.
73. Nikos Theodorakopoulos and M Peyrard. Solitons and nondissipative diffusion. *Physical review letters*, 83(12):2293, 1999.
74. Herbert Spohn. Interacting and noninteracting integrable systems. *Journal of Mathematical Physics*, 59(9):091402, 2018.
75. Aritra Kundu and Abhishek Dhar. Equilibrium dynamical correlations in the Toda chain and other integrable models. *Phys. Rev. E*, 94:062130, Dec 2016.
76. Pierfrancesco Di Cintio, Stefano Iubini, Stefano Lepri, and Roberto Livi. Transport in perturbed classical integrable systems: The pinned Toda chain. *Chaos, Solitons & Fractals*, 117:249–254, 2018.

77. Abhishek Dhar, Aritra Kundu, Joel L. Lebowitz, and Jasen A. Scaramazza. Transport properties of the classical Toda chain: Effect of a pinning potential. *Journal of Statistical Physics*, 175(6):1298–1310, Jun 2019.
78. Alessandra Iacobucci, Frederic Legoll, Stefano Olla, and Gabriel Stoltz. Thermal conductivity of the Toda lattice with conservative noise. *Journal of Statistical Physics*, 140(2):336–348, Jul 2010.
79. Shunda Chen, Jiao Wang, Giulio Casati, and Giuliano Benenti. Nonintegrability and the Fourier heat conduction law. *Phys. Rev. E*, 90:032134, Sep 2014.
80. Alessandro Campa, Thierry Dauxois, Duccio Fanelli, and Stefano Ruffo. *Physics of long-range interacting systems*. OUP Oxford, 2014.
81. Ricardo R Avila, Emmanuel Pereira, and Daniel L Teixeira. Length dependence of heat conduction in (an) harmonic chains with asymmetries or long range interparticle interactions. *Physica A: Statistical Mechanics and its Applications*, 423:51–60, 2015.
82. Debarshee Bagchi. Thermal transport in the Fermi-Pasta-Ulam model with long-range interactions. *Phys. Rev. E*, 95(3):032102, 2017.
83. Carlos Olivares and Celia Anteneodo. Role of the range of the interactions in thermal conduction. *Phys. Rev. E*, 94:042117, 2016.
84. Stefano Iubini, Pierfrancesco Di Cintio, Stefano Lepri, Roberto Livi, and Lapo Casetti. Heat transport in oscillator chains with long-range interactions coupled to thermal reservoirs. *Phys. Rev. E*, 97:032102, Mar 2018.
85. P Di Cintio, S Iubini, S Lepri, and R Livi. Equilibrium time-correlation functions of the long-range interacting Fermi–Pasta–Ulam model. *Journal of Physics A: Mathematical and Theoretical*, 52(27):274001, jun 2019.
86. David Ruelle. *Statistical mechanics: Rigorous results*. World Scientific, 1999.
87. Lev Vidmar and Marcos Rigol. Generalized Gibbs ensemble in integrable lattice models. *Journal of Statistical Mechanics: Theory and Experiment*, 2016(6):064007, 2016.

